ELSEVIER

Catalysis Today 52 (1999) 91–98

CATALYSIS TODAY

Towards understanding the enhanced cracking activity of steamed Y zeolites

H.H. Kung[a,*], B.A. Williams[a], S.M. Babitz[a], J.T. Miller[b], R.Q. Snurr[a]

[a]*Department of Chemical Engineering, Northwestern University, 2145 Sheridan Road, Evanston, IL 60208-3120, USA*
[b]*Amoco Chemicals, PO Box 3011, Mail Station E-1F, Naperville, IL 60566-7011, USA*

Abstract

Ultrastable Y (H-USY) zeolite, prepared by steam treatment of Y zeolite, is a very active hydrocarbon cracking catalyst. However, the extent of enhancement in activity compared to a non-steamed sample depends on the reaction condition. A model that has been proposed to explain this behavior is summarized. The model incorporates the three different mechanisms for hydrocarbon cracking, and the dependence of their rates on the partial pressures of reactants and products and temperature. Depending on the reaction condition, such as hydrocarbon pressure, temperature, and conversion, the predominant cracking reaction mechanism may differ. The change in the predominant mechanism may also be a result of the proportionally small increase in external surface area caused by the steaming-induced structural destruction of the zeolite particles. However, these relatively small changes can lead to a much larger overall effect on the cracking rate because of the sensitive dependence of oligomeric cracking, and to a lesser extent, bimolecular cracking on the alkene partial pressure. © 1999 Elsevier Science B.V. All rights reserved.

Keywords: Zeolites; Cracking activity; Steam treatment; Ultrastable Y

1. Introduction

Catalytic hydrocarbon cracking is an important step in the conversion of crude oil to transportation fuels. Industrial cracking catalysts contain a significant component resembling an H-USY zeolite, and it is generally accepted that the cracking activity can be attributed to the Brønsted acidity of the zeolite. H-USY zeolite can be prepared by hydrothermal treatment of zeolite Y. This process results in a number of structural changes that have been well documented in the literature. First, destruction of part of the zeolite framework occurs. Electron microscopy studies of steamed Y zeolites have shown the presence of a substantial number of mesopores, cracks and fissures [1,2]. Second, some framework aluminium (Al_F) ions are removed from the zeolite structure and exist as extra-framework aluminum (Al_{EF}) species, some of which can be identified by NMR as octahedrally-coordinated Al ions [3–6]. Finally, new Lewis acid sites and hydroxyl groups appear that can be monitored spectroscopically [7] and calorimetrically [8–10].

The catalytic consequence of steaming is that the zeolite can become much more active for cracking, sometimes by nearly two orders of magnitude compared to unmodified catalysts. The enhancement in activity depends on the pretreatment of the sample,

---

*Corresponding author.

PII: S0920-5861(99)00066-8

such as the method and severity of the steaming process, in addition to the concentration of Al_F in the original sample [11–13]. Since commercial cracking catalysts contain USY zeolites, it has been of great scientific interest and commercial value to understand the origin of the enhanced activity.

The most widely accepted explanation of the enhanced activity is the special site model [14], which assumes that, as a result of the steaming or dealumination process, unusually active sites that are also unusually strong Brønsted acid sites are produced. A second explanation assumes that the cracking reaction in HY and H-USY zeolite is pore-diffusion limited [15]. Mesopores, crevices and fissures formed during the dealumination process increase the external surface area of the zeolite particles for diffusion, and, consequently, the activity of the steamed catalyst. A third explanation involving the participation of Lewis acid centers for initiation reactions [16,17] is inconsistent with recent experimental observations and has not found general acceptance [18,19]. It will not be explicitly discussed further.

There are many experimental observations that can be interpreted by the widely accepted acid strength model (for a summary of these observations, see [20]). Some, such as a large decrease in cracking activity by poisoning a relatively small fraction of acid sites, have been considered strong evidence supporting the special site model [21], and there are spectroscopic evidence of stronger interaction of the new hydroxyl groups with probe molecules, which implies stronger acids [22,23]. Nonetheless, there has been no direct detection of sites that are unusually active and strongly acidic. On the other hand, there are observations that do not support this model. For example, correlations between acid strength and cracking activity over dealuminated Y zeolites are, at best, qualitative [12]. Also, the effect of Al_{EF} on cracking activity in steamed zeolites seems to be unclear, although it has been cited as a dominant factor influencing Brønsted acid strength [12,24,25]. Very importantly, it was reported recently that for hexane cracking on a H-USY, a chemically dealuminated Y(CDHY), and a H-ZSM-5 zeolite (Table 1), the intrinsic activation energy was the same within experimental uncertainties, when measured under conditions when the monomolecular cracking mechanism dominates [26]. That is, the differences in the apparent activation energies among

Table 1
Kinetics of *n*-hexane cracking (from [26]; experimental condition: 380 Pa purified hexane in nitrogen, 480–540°C)

Sample	Temperature (°C)	TOF (molecule/site-s)×10^5		E_{obs} (kJ/mol)	ΔH_{ads} (kJ/mol)	E_{int}[a] (kJ/mol)
		(AlF-Na)[c]	$\Delta H_{NH3} \geq 90$ (kJ/mol)			
HZSM-5	480	75.7	91			
	500	122	152			
	520	232	293			
	540	365	460			
				149±8	−86±6	235±14
H-USY	480	6.8	11.0			
	500	12.5	20.5			
	520	26.9	44.2			
	540	49.1	79.8			
				177±9	−50±3	227±12
CDHY[b]	480	3.4	4.3			
	500	5.7	7.2			
	520	11.0	14.4			
	540	19.0	23.9	186±9	−50±3	236±12

[a] $E_{int}=E_{obs}-\Delta H_{ads}$.

[b] HY dealuminated by ammonium hexafluorosilicate.

[C] Na/tetrahedral Al per unit cell ratios are: H-USY: 0.5/28, CDHY: 0.25/26; HZSM-5: 0.09/3.7.

Table 2
Initial product selectivities in hexane cracking (mol%; from [26], experimental conditions as in Table 1)

Product	H-ZSM-5	H-USY	CHDY
H_2	17	22	12
CH_4	4	6	7
C_2H_6	13	11	12
C_2H_4	5	4	6
C_3H_8	12	10	11
C_3H_6	30	29	35
i-C_4H_{10}	0.0	0.0	0.0
n-C_4H_{10}	2	3	3
C_4H_8	17	12	12
i-C_5H_{12}	0.4	2	1
Total	100	100	100

the three zeolites can be accounted for by the differences in their heats of adsorption of the hexane. The turnover frequencies are very similar between the two Y zeolites also, an observation that is very different from when they are measured under conditions when the predominant mechanism is not monomolecular [27]. In addition, the product distributions are very similar (Table 2), confirming that the same reaction mechanism operated in testing these catalysts.

In the monomolecular cracking mechanism, the rate-limiting step is believed to be protonation of the hydrocarbon to form a high energy transition state that has a five-coordinated carbon like a carbonium ion [28,29], which should be sensitive to the strength of the proton acid. Thus, this observation suggests that there are no differences in the acid strengths among these three zeolites, or that the difference in acid strength is not important under these conditions.

Likewise, only indirect evidence supporting the diffusion model has been reported [15,30]. Recently, a new model has been proposed that appears to be able to explain a wider range of literature observations [20]. This model differs from the others in that it takes into account explicitly the existence of different reaction mechanisms for cracking, and that the relative contributions of the various mechanisms to the overall observed rate depend on experimental conditions, especially alkane conversion, temperature, and olefin partial pressure. In this paper, a summary of the new model is presented, together with a discussion of it with respect to various experimental observations.

2. Cracking reaction mechanism

In the literature, it has been proposed that hydrocarbon cracking operates via two mechanisms: monomolecular and bimolecular [16,28]. Recently, a refinement was proposed by subdividing the reactions in the previous bimolecular mechanism into bimolecular and oligomeric cracking [20]. The last one was introduced to explicitly account for deactivation by coke and for the formation of products larger in carbon number than the feed molecule.

2.1. Monomolecular cracking

An alkane molecule is protonated (Eq. (1)) to form a non-classical penta-coordinated carbonium ion (also known as an alkanium ion [31]) as the high-energy transition state [28,29]. It should be emphasized that the carbonium ion is strongly coordinated to the surface lattice oxygen, such that it is not a free ion. The lattice oxygen ions are explicitly shown in Eq. (1), but will be omitted in later equations.

$$\text{Protonation}: \quad CR_2H_2 + H^+ - ZO^- \rightarrow [CR_2H_3^+] - ZO^- \qquad (1)$$

$$\text{Dehydrogenation}: \quad [CR_2H_3^+] \rightarrow CR_2H^+ + H_2 \qquad (2)$$

$$\text{Cracking}: \quad [CR_2H_3^+] \rightarrow RH + CRH_2^+ \qquad (3)$$

$$\text{Desorption}: \quad CR_2H^+ \rightarrow \text{alkane} + H^+ \qquad (4)$$

$$CRH_2^+ \rightarrow \text{alkene} + H^+ \qquad (5)$$

This mechanism describes the slow initiation steps for the cracking of pure alkane when it comes in contact with a clean zeolite surface. The activation energy is high because of the high energy transition state ($[CR_2H_3^+] - ZO^-$) complex, and it is reasonable to assume that the rate of formation of this transition state is directly related to the acid strength of a Brønsted proton. Thus, stronger acid sites are expected to be proportionally more active. Dehydrogenation (Eq. (2)) or cracking (Eq. (3)) of the carbonium ion results in the formation of dihydrogen or smaller alkanes and an alkene, which may be adsorbed as a carbenium ion that is also strongly coordinated to the surface. Theoretical calculations [29,32] and experimental results [33,34] have shown that steps (1)–(3) occur as a concerted process. The adsorbed carbenium ion (which may be more appropriately described as a σ-bonded alkoxy group [32]) may desorb as an alkene as shown in reactions (4) and (5), or undergo secondary β-scission by reaction (9) to form smaller alkenes and adsorbed carbenium ions. This pathway should be favored at high temperatures, low hydrocarbon partial pressures, and low conversions.

2.2. *Bimolecular cracking*

In this mechanism, a reactant alkane undergoes hydride transfer (H-transfer) with an adsorbed carbenium ion (reaction 7). The resulting carbenium ion undergoes isomerization (reaction 8) and/or β-scission (reaction 9).

$$\text{Initiation}: \quad \mathrm{H}^+ + \text{alkene} \rightarrow \mathrm{R}_j^+ \tag{6}$$

$$\mathrm{H-transfer}: \quad \mathrm{R}_i\mathrm{H} + \mathrm{R}_j^+ \rightarrow \mathrm{R}_i^+ + \mathrm{R}_j\mathrm{H} \tag{7}$$

$$\text{Isomerization}: \quad \mathrm{R}_i^+ \rightarrow \mathrm{R}_{i'}^+ \tag{8}$$

$$\beta - \text{scission}: \quad \mathrm{R}_i^+ \rightarrow \text{alkene} + \mathrm{R}_j^+ \quad (j < i) \tag{9}$$

This process may begin by step (6) which involves alkene adsorption on a Brønsted proton. The origin of the initial alkenes may be either the monomolecular cracking reactions or as impurities in the alkane reactant. Once initiated, this pathway may be up to 800 times faster, with a much lower activation energy, than the monomolecular reaction [35]. It is favored at lower temperatures and higher partial pressures of alkene, when higher carbenium ion coverages are obtained, and which occurs at higher conversions [28,36]. Because of the fast rate, this pathway is likely controlled by diffusion in the micropores of a zeolite. That is, the observed rate would depend on the external surface area of the zeolite particle, which is higher for steamed particles that have mesopores, crevices and fissures. This process is autocatalytic, since higher alkane conversion produces more alkene, which increases the carbenium ion coverage, and thus alkane conversion by reactions (7) and (9) [28]. The rate of the H-transfer reaction (7), because it involves a carbenium ion and an alkane, would be expected to be less sensitive to the strength of the acid site than the monomolecular reaction. Additionally, at low surface coverages of carbenium ions, the bimolecular process would be first order in alkene partial pressure.

2.3. *Oligomeric cracking*

This mechanism is introduced as a distinct one to explicitly account for deactivation by coke and the formation of products larger in carbon number than the feed. It is similar to bimolecular cracking except that the H-transfer step occurs between the reactant alkane ($\mathrm{R}_i\mathrm{H}$) and an oligomeric surface carbenium ion (R_m^+), which is formed by alkylation of a smaller carbenium ion (R_j^+ or R_n^+).

$$\text{Alkylation}: \quad \text{alkene} + \mathrm{R}_n^+ \rightarrow \mathrm{R}_m^+ \tag{10}$$

$$\text{H-transfer}: \quad \mathrm{R}_i\mathrm{H} + \mathrm{R}_m^+ \rightarrow \mathrm{R}_i^+ + \mathrm{R}_m\mathrm{H} \tag{11}$$

$$\text{H-transfer}: \quad \mathrm{R}_m\mathrm{H} + \mathrm{R}_p^+ \rightarrow \mathrm{R}_m^+ + \mathrm{R}_p\mathrm{H} \tag{11a}$$

$$\text{Isomerization}: \quad \mathrm{R}_i^+ \rightarrow \mathrm{R}_p^+ \tag{12}$$

$$\beta - \text{scission}: \quad \mathrm{R}_i^+ \rightarrow \text{alkene} + \mathrm{R}_j^+ \tag{13}$$

$$\beta - \text{scission}: \quad \mathrm{R}_m^+ \rightarrow \text{alkene} + \mathrm{R}_n^+ \tag{13a}$$

Here, $j \leq n < m$, $j < i$, and p have any value in these equations. In this mechanism, the alkylation or oligomerization step (Eq. (10)) is favored by high alkene partial pressure and high surface carbenium ion concentration (which occur at high conversions). Alkane conversion proceeds via an H-transfer/β-scission cycle (Eqs. (11)–(13) and (13a)). Unlike bimolecular cracking, the alkane ($\mathrm{R}_m\mathrm{H}$) formed in the H-transfer step (Eq. (11)) may remain adsorbed on the surface because of its high molecular weight (i.e. low vapor pressure) [36], and undergo further H-transfer with other carbenium ions of any size (Eq. (11a)), such that there is little depletion of the surface oligomer concentration. Therefore, the overall rate constant per unit catalyst volume for alkane conversion by this mechanism should be at least as large as, and likely larger than that for the bimolecular cracking reaction [37–39]. The rate of alkane conversion by H-transfer (Eq. (11)) depends on the coverage of oligomeric surface carbenium ions, which is proportional to the alkylation rate as a first approximation. Since the alkylation rate depends on the product of alkene partial pressure and the surface carbenium ion concentration (a term that also depends on alkene partial pressure), the oligomeric cracking rate would have a higher order dependence on the alkene partial pressure than bimolecular cracking. Because of the large rate constant, step (10) and possibly step (11) are most likely micropore diffusion limited when the alkane conversion is not too small, and the overall rate would depend on the external surface area of the zeolite [40]. As with bimolecular cracking, the oligomeric process is autocatalytic. Higher conversions enhance the alkylation reaction (Eq. (10)), thereby increasing the number of sites for H-transfer with the reactant by step (11) [28]. Coke deposition occurs when the alkylation step is faster than the scission step, such that the size of the surface oligomer continues to grow and eventually cyclizes to form aromatic coke [38]. As with the bimolecular mechanism, this pathway is expected to be less sensitive to the strength of an acid site than the monomolecular cracking reaction.

3. Reaction model

At the beginning of the reaction (i.e. very short time-on-stream (TOS)), a pure alkane feed comes in contact with a clean zeolite at the reactor inlet. The only possible reaction is monomolecular cracking on Brønsted acid sites. An important consequence of this reaction is that some adsorbed carbenium ions are formed, the desorption of which results in the appearance of small amounts of alkene in the gas phase. The alkene molecules travel down the reactor bed and are readsorbed on Brønsted sites to form carbenium ions, which undergo bimolecular H-transfer with reactant alkane and cracking. This is a cumulative effect down the catalyst bed, and the conversion of alkane increases quite rapidly due to the increased olefin production, surface carbenium ion concentration, and therefore, participation of bimolecular cracking, as shown in Fig. 1. This non-linearity between residence time and catalyst activity has been addressed in the literature as the autoacceleration of an integral flow reactor [38,41,42] or the inhibition time for a batch reactor [43]. Further down the catalyst bed, once a sufficient alkene partial pressure is established, alkylation and oligomeric cracking become significant, further accelerating the rate of feed conversion (Fig. 1). In turn, the participation of oligomeric cracking leads to even higher observed alkane conversion, and deactivation of the catalyst by coking begins to occur. At this point, the majority of the observed alkane conversion would be due to the oligomeric cracking reaction. Up to this point, broadly speaking, the description here has some similarities to those described by Dumesic and coworkers [44–47].

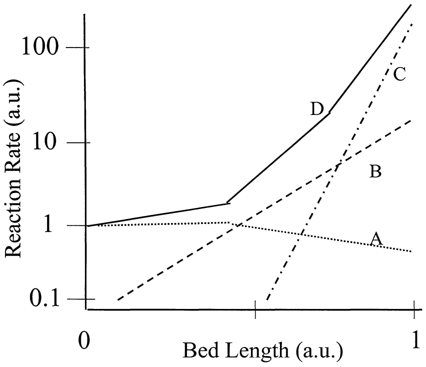

Fig. 1. A schematic drawing of the contributions of monomolecular (A), bimolecular (B) and oligomeric (C) cracking to the overall activity (D) as a function of position along the catalyst bed at short time-on-stream.

Implicit in this description is that the relative contributions of the three mechanisms to the overall observed reaction depends on the reaction conditions. In particular, they depend on the alkane partial pressure and conversion, which affect the olefin concentration. Thus, implicitly, they depend on the space velocity. They also depend on the temperature, which affects the adsorption of olefin on the zeolite. In general, higher temperatures, shorter residence times or lower conversions, and lower alkane partial pressures, and weaker adsorption of the corresponding olefins (i.e. smaller hydrocarbons) tend to favor monomolecular cracking that does not deactivate the catalyst, whereas the opposite conditions favor oligomeric cracking, which causes deactivation.

With increasing time-on-stream, the catalyst deactivates by coking. According to this model, coke formation is due to alkylation and chain growth, which is a reaction step in the oligomeric cracking mechanism. Thus, it occurs in the portion of the catalyst bed where oligomeric cracking is significant. The model predicts further that as a catalyst bed becomes increasingly, deactivated, monomolecular cracking becomes an increasingly important contributor to the remaining catalytic activity.

Experimental observations are in support of this description. In the cracking of 2-methylpentane, the ratio of propane and propene products (used to indicate monomolecular cracking) to isobutane and iso-

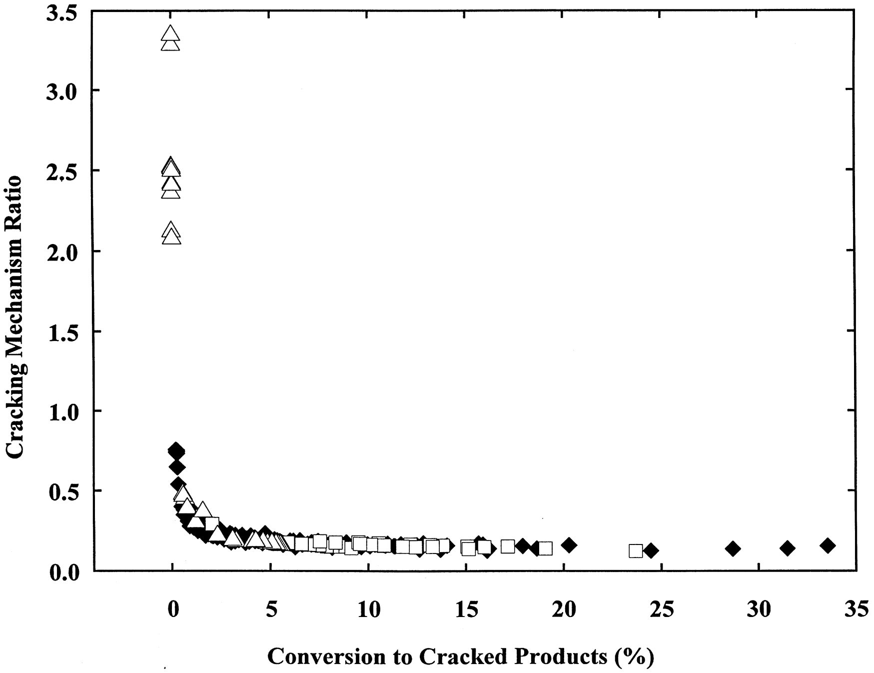

Fig. 2. Ratio of $(C_3 + C_3^=)/(i\text{-}C_4 + i\text{-}C_4^=)$, as a function of 2-methylpentane conversion to cracked products at 573 K over HY (△), CHDY (□), and H-USY (◆) zeolites. Each point represents the instantaneous conversions and product selectivities at various times-on-stream between 1 and 110 min for 22 independent reaction runs. Each run was carried out at 300°C with a nitrogen carrier gas stream saturated with 2-methylpentane at 273 K.

butene (used to indicate bimolecular and oligomeric cracking) is a much more sensitive function of the alkane conversion than other variables, including time-on-stream or the type of zeolite (Fig. 2). Although the exact relationship between these products and the reaction mechanism still needs to be clarified, the product distribution can be used qualitatively as an indication of whether the same mechanism dominates in a reaction. The correlation observed in Fig. 2 indicates that, in accordance with the model presented, the relative contributions of various reaction mechanisms depend primarily on the alkane conversion, given identical reaction conditions. A similar observation has been reported by others [48], although the data were interpreted differently.

Using this model, the effect of steaming of a zeolite can be interpreted as follows. Without steaming to generate the mesopores, crevices or fissures, most of the Brønsted acid sites in HY are inaccessible to the micropore diffusion-limited bimolecular and oligomeric cracking reactions. Defects generated by steaming increase the external surface area, and the contributions of the fast bimolecular and oligomeric cracking reaction increase correspondingly. The magnitude of this effect on the observed overall reaction rate can be illustrated by the comparison shown in Table 3 for each mechanism. In this table, it is assumed that both the bimolecular and oligomeric cracking reactions are strongly diffusion-limited, such that their rate constants per unit volume of the catalyst are proportional to the external surface area of the zeolite crystal. As discussed earlier, the bimolecular reaction is first-order, and the oligomeric reaction is second-order in olefin partial pressure, which is assumed to be proportional to the alkane conversion. Finally, the relative changes in the overall reaction rate is proportional to the product of these changes. For example, a threefold increase in external surface area would triple the rate constant per unit volume for the H-transfer/β-scission cycle, which results in proportionally higher alkene production. The relative overall reaction rate is then increased by a factor of 9 and

Table 3
Effect of external surface area on hydrocarbon cracking rates

Rates	Base case	External surface area increase	
		×2	×3
Monomolecular cracking	1	1	1
Bimolecular cracking	1		
Rate constant (per unit volume)		2	3
Total rate:↑ (rate constant)×↑ [alkene]		4	9
Oligomeric cracking	1		
Rate constant (per unit volume)		2	3
Total rate: ↑ (rate constant)×↑ $[\text{alkane}]^2$		8	27

27 for bimolecular and oligomeric cracking, respectively.

Although the quantitative aspects of this table need to be confirmed by experiments, the qualitative conclusions are clear. It illustrates how, under conditions where bimolecular and oligomeric cracking dominate, the overall alkane conversion rate can be enhanced very significantly by much smaller changes in the catalyst external surface area. It also shows how the activity enhancement due to steaming depends on the nature of the alkane, the extent of deactivation of the catalyst, and the process conditions such as temperature, reactant partial pressure, residence time, and time-on-steam.

Experimental evidence to support this model is being gathered. The transition from a first-order to a higher-order kinetics as the hexane partial pressure increases from 130 to 700 Pa or higher at 400°C has been observed in our laboratory. At the higher pressures, deactivation also becomes apparent. According to the model, this transition is due to the change from monomolecular cracking being the dominant reaction mechanism to bimolecular/oligomeric cracking.

This model can be used to describe the effect of selective site poisoning also [21,49,50]. Poisoning of a small portion of the active sites, especially if they are close to the micropore mouths, would have a disproportionately large effect on the bimolecular and oligomeric cracking rates. Under the conditions where these mechanisms contribute significantly to the observed conversion, a decrease in the rates of these reactions would have a multiplying effect at the latter part of the catalyst bed, because of slower build-up of olefin partial pressure, resulting in a much more pronounced decrease in the observed overall cracking activity. The net result is an appearance of selective site poisoning.

Finally, the diffusional influence on cracking rates have been demonstrated experimentally for larger molecules [51,52]. The model presented here suggests that it can be important for smaller molecules also under conditions when the very fast bimolecular/oligomeric cracking are important. Most importantly, the model recognizes the fact that the role of diffusion depends on the dominant mechanism, which in turn depends on the experimental conditions.

4. Conclusion

A reaction model is described as an alternate explanation of observation in the literature concerning the effect of steaming on hydrocarbon cracking reaction over zeolites, particularly zeolite Y. The model incorporates the relative rates of various reaction pathways known to participate in the cracking reaction, the effect of micropore diffusion limitation, and the effect of adsorption equilibrium on the fast bimolecular and oligomeric cracking reactions. It explains how small changes in these can generate a much larger effect on the observed overall alkane conversion because of the sensitive dependence of the oligomeric cracking rate, and to a lesser extent, the bimolecular cracking rate, on the alkene partial pressure and the alkane conversion. It also accounts for changes observed during catalyst deactivation and selective site poisoning.

Acknowledgements

Financial support from the National Science Foundation, Division of Chemical and Thermal Systems, and many helpful discussions, with Dr. W.O. Haag are gratefully acknowledged.

References

[1] V. Patzelova, N.I. Jaeger, Zeolites 7 (1987) 240.

[2] C. Choi-Feng, J.B. Hall, B.J. Huggins, R.A. Beyerlein, J. Catal. 140 (1993) 395.

[3] J. Klinowski, J.M. Thomas, C.A. Fyfe, G.C. Gobbi, Nature 296 (1982) 533.

[4] J. Klinowski, C.A. Fyfe, G.C. Gobbi, J. Chem. Soc., Faraday Trans. 81 (1985) 3003.

[5] A. Samoson, E. Lippmaa, G. Engelhardt, U. Lohse, H.-G. Jerschkewitz, Chem. Phys. Lett. 134 (1987) 589.

[6] J. Sanz, V. Forne, A. Corma, J. Chem. Soc., Faraday Trans. 84 (1988) 3113.

[7] A. Janin, J.C. Lavalley, A. Macedo, F. Raatz, in: W.H. Flank, T.E. Whyte Jr. (Eds.), Perspectives in Molecular Sieve Science, American Chemical Society, Symposium Series no.368, Washington, DC, 1988, p. 177.

[8] A. Auroux, Y. Ben Taarit, Thermochim. Acta 122 (1987) 63.

[9] A.I. Biaglow, D.J. Parrillo, G.T. Kokotailo, R.J. Gorte, J. Catal. 148 (1994) 213.

[10] D. Chen, S. Sharma, N. Cardona-Martinez, J.A. Dumesic, V.A. Bell, G.D. Hodge, R.J. Madon, J. Catal. 136 (1992) 392.

[11] F. Lonyi, J.H. Lunsford, J. Catal. 136 (1992) 566.

[12] R.A. Beyerlein, G.B. McVicker, L.N. Yacullo, J.J. Ziemak, J. Phys. Chem. 92 (1988) 1967.

[13] P.V. Shertukde, W.K. Hall, J.-M. Dereppe, G. Marcelin, J. Catal. 139 (1993) 468.

[14] J.H. Lunsford, in: M.L. Occelli (Ed.), Fluid Catalytic Cracking 11: Concepts in Catalyst Design, American Chemical Society Symposium Series no. 452, Washington, DC, 1991, p. 1.

[15] P.D. Hopkins, J.T. Miller, B.L. Meyers, G.J. Ray, R.T. Roginski, M.A. Kuehne, H.H. Kung, Appl. Catal. A 136 (1996) 29.

[16] A. Corma, J. Planelles, J. Sanchez-Marin, F. Tomas, J. Catal. 93 (1985) 30–37.

[17] V.L. Zholobenko, L.M. Kustov, V.B. Kazansky, E. Loeffler, U. Lohser, G. Oehlmann, Zeolites 11 (1991) 132.

[18] J.W. Ward, J. Catal. 11 (1968) 238.

[19] S.M. Babitz, M.A. Kuehne, H.H. Kung, J.T. Miller, Ind. Eng. Chem. Res. 36 (1997) 3027.

[20] B.A. Williams, S.M. Babitz, J.T. Miller, R.Q. Snurr, H.H. Kung, Appl. Catal. A 177 (1999) 161.

[21] P.O. Fritz, J.H. Lunsford, J. Catal. 118 (1989) 85.

[22] M.A. Makarova, K.M. Al-Ghefaili, J. Dwyer, J. Chem. Soc., Faraday Trans. 90 (1994) 383.

[23] M.A. Makarova, S.P. Bates, J. Dwyer, J. Am. Chem. Soc. 117 (1995) 11309.

[24] G.R. Bamwednea, Y.X. Zhao, W.A. Groten, B.W. Wojciechowski, J. Catal. 150 (1994) 243.

[25] G.R. Bamwednea, Y.X. Zhao, W.A. Groten, B.W. Wojciechowski, J. Catal. 157 (1995) 209.

[26] S.M. Babitz, B.A. Williams, J.Y. Miller, R.Q. Snurr, W.O. Haag, H.H. Kung, Appl. Catal. A 179 (1999) 71.

[27] M.A. Kuehne, S.M. Babitz, H.H. Kung, J.T. Miller, Appl. Catal. A 166 (1998) 293.

[28] W.O. Haag, R.M. Dessau, in: Proceedings of the Eighth International Congress on Catalysis, vol. 2, Verlag-Chemie, Weinheim, 1984, p. 305.

[29] S.R. Blaszkowski, R.A. van Santen, Topics Catal. 4 (1997) 145.

[30] K.P. Moller, M. Kojima, C.T. O'Connor, Chem. Eng. J. 54 (1994) 115.

[31] G.P. Moss, P.A.S. Smith, D. Tavernier, Pure Appl. Chem. 67 (1995) 1307.

[32] V.B. Kazanski, I.W. Senchenya, J. Catal. 119 (1989) 108.

[33] T.F. Narbeshuber, H. Vinek, J.A. Lercher, J. Catal. 157 (1995) 388.

[34] H. Krannila, W.O. Haag, B.C. Gates, J. Catal. 135 (1992) 115.

[35] W.O. Hagg, R.M. Lago, P.B. Weisz, Faraday Disc. 72 (1982) 317.

[36] P. Voogd, H. Van Bekkum, Appl. Catal. 59 (1990) 311.

[37] W.O. Hagg, in: Weitkamp et al. (Eds.), Zeolites and Related Microporous Materials: State of the Art 1994, Studies in Surface Science and Catalysis, no. 84, Elsevier, Amsterdam, 1994, p. 1375.

[38] K.A. Cumming, B.W. Wojciechowski, Catal. Rev.-Sci. Eng. 38 (1996) 101.

[39] W.O. Hagg, R.M. Dessau, R.M. Lago, in: Chemistry of Microporous Crystals: Studies in Surface Science and Catalysis, no. 60, Elsevier, Amsterdam, 1991, p. 255.

[40] S.J. Miller, in: J.W. Ward (Ed.), Catalysis 1987, Studies in Surface Science and Catalysis, no. 38, Elsevier, Amsterdam, 1988, p. 199.

[41] E. Dempsey, J. Catal. 33 (1974) 497.

[42] E. Dempsey, J. Catal. 39 (1975) 155.

[43] L. Riekert, J.-Q. Zhou, J. Catal. 137 (1992) 437.

[44] G. Yaluris, R.J. Madon, J.A. Dumesic, Ind. Eng. Chem. Res. 33 (1994) 2913.

[45] G. Yaluris, R.J. Madon, J.A. Dumesic, J. Catal. 153 (1995) 54.

[46] G. Yaluris, R.J. Madon, J.A. Dumesic, J. Catal. 153 (1995) 65.

[47] G. Yaluris, R.J. Madon, J.A. Dumesic, J. Catal. 165 (1997) 205.

[48] N.P. Rhodes, R. Rudham, N.H.J. Standbridge, J. Chem. Soc., Faraday Trans. 92 (1996) 2817.

[49] J. Engelhardt, W.K. Hall, J. Catal. 125 (1990) 472.

[50] R.A. Beyerlein, G.B. McVicker, L.N. Yacullo, J.J. Ziemak, Prep. Div. Pertol. Chem., Am. Chem. Soc. 31 (1986) 190.

[51] M.A. Camblor, A. Corma, A. Martínez, F.A. Mocholí, J. Pérez Parientí, Appl. Catal. 55 (1989) 65.

[52] K. Rajagopalan, A.W. Peters, G.C. Edwards, Appl. Catal. 23 (1989) 69.